UNIVERSITY OF WEST BOHEMIA

Applied and Computational Mechanics 3 (2009) 363–374

Applied and Computational Mechanics

Glass fibre reinforced cement based composite: fatigue and fracture parameters

S. Seitl[a,*], Z. Keršner[b], V. Bílek[c], Z. Knésl[a]

[a] *Institute of Physics of Materials, Academy of Sciences of the Czech Republic, v.v.i., Žižkova 22, 616 62 Brno, Czech Republic*

[b] *Institute of Structural Mechanics, Civil Engineering Faculty, Brno University of Technology, Veveří 331/95, 602 00 Brno, Czech Republic*

[c] *ZPSV, a.s., Testing laboratory Brno, Křižíkova 68, 660 90 Brno, Czech Republic*

Received 28 August 2009; received in revised form 2 December 2009

Abstract

This paper introduces the basic fracture mechanics parameters of advanced building material – glass fibres reinforced cement based composite and its fracture and fatigue behaviour is investigated. To this aim three-point bend (3PB) specimens with starting notch were prepared and tested under static (l–d diagram) and cyclic loading (Paris law and Wöhler curve). To evaluate the results, the finite element method was used for estimation of the corresponding values of stress intensity factor for the 3PB specimen used. The results obtained are compared with literature data.

Keywords: cement based composite, glass fibre, effective fracture toughness, Paris law, S–N curve

1. Introduction

In recent years, interest has risen concerning the behaviour of high-strength/high-performance concrete subjected to fatigue loading can be observed because of its frequent use in structures such as long-span bridges, offshore structures and reinforced concrete pavements.

Fatigue is a process of progressive and permanent internal damage in materials subjected to repeated loading. This is attributed to the propagation of internal micro-cracks that may result in the propagation of macro-cracks and unpredictable failure. Fatigue phenomena related to metallic structures have been analyzed since the 19th century (for instance, see book by Suresh [20] for review), whereas the behaviour of reinforced/concrete (RC) structures under cyclic loading has been studied for only a few decades (see article by Lee and Barr [9], for review). Concrete is a highly heterogeneous material and the processes operating in its structure and leading to its degradation under cyclic loading are more complicated in comparison with these in metals. The fatigue mechanism may be attributed to progressive bond degradation between coarse aggregates and the cement paste or by development of cracks existing in the cement paste. Similarly to metals, the process leading to fatigue failure caused by macro-crack propagation consists of three phases. The first one is connected with crack initiation and typically takes place in the vicinity of stress concentrators in the weaker phase(s) of the microstructure. The second phase is characterized by the stable growth of the initiated crack up to its critical length. The final part is associated with unstable growth of the macro-crack and leads to the final fracture (usually of brittle type) of the structure. With regard to the service life

*Corresponding author. Tel.: +420 532 290 348, e-mail: seitl@ipm.cz.

Table 1. Classes of fatigue load, initiate (by Lee and Barr [9])

Low-cycle fatigue			High-cycle fatigue				Super-high-cycle fatigue		
1	10^1	10^2	10^3	10^4	10^5	10^6	10^7	10^8	10^9
Structures subjected to earthquakes			Airport pavements and bridges		Highway and railway bridges, highway pavements		Mass rapid transit structure		Sea structures

of the structure, the most important is the second part which represents up to 80 % of the total life cycle. Quantification of the crack behaviour in this phase is of paramount importance.

Fatigue loading is usually divided into three categories, i.e. low-cycle, high-cycle loading and super-high-cycle fatigue. Table 1 summarizes the different classes of fatigue loading that Lee and Barr published in their overview article [9]. It is supposed that the studied material is intended for using in high cycle fatigue region.

Based on linear elastic fracture mechanics concepts, various fatigue crack propagation laws have been proposed. In the 1980s, Baluch et al. [3] and Perdikaris and Calomino [12] reported that Paris' law [11] is a useful method for characterizing the stable fatigue crack growth behaviour of concrete. A more sophisticated propagation law, including loading history and specimen size, has been suggested by e.g. Slowik et al. [19]. Experimental fatigue crack growth data for normal (Bazant and Xu in [5]) and high strength (Bazant and Shell in [4]) concrete show that, for a given value of the stress intensity factor range, crack growth rate decreases by increasing the structural size.

The aim of the paper is to present selected fatigue and fracture mechanics parameters of advanced building materials marked here as BS 080405. The experimental measurements were made at two levels. The first one was a static measurement and its results are represented by values of effective fracture toughness of the material. The second level is connected with stable fatigue crack propagation under cyclic loading. For this purpose, fatigue crack propagation rate was determined on a three-point bend specimen and correlated with the applied stress intensity factor range ($\mathrm{d}a/\mathrm{d}N$–ΔK curve) corresponding to simple Paris law. To complete basic fatigue parameters of the materials a Wöhler curve was determined. Note that the paper is connected with and expands the paper of co-authors Seitl et al. [14] that was published on the 8th HSC–HPC SYMPOSIUM.

2. Material and Methods of Measurement

In this section the material and methodology used in this paper are introduced.

2.1. Material BS 080405

The specimens tested were prepared as high performance concrete/mortar developed by ZPSV, a.s., company for production of thin-walled panels/elements. The dosage of cement CEM I 42.5R Mokra was 1 000 kg per m^3 of fresh mixture, water to cement ratio was 0.28, superplasticizer Spolostan; sand aggregates of 4 mm maximum size were used. Alkali-resistant glass fibres (glass with high content of zirconium oxide) are applied with a dosage of 5 kg per m^3 of fresh mixture (0.2 %). Properties of fibres were as follows: tensile strength 3 500 MPa, modulus of elasticity 73 GPa, diameter 14 μm, length 12 mm. The feature of the investigated specimens fracture surface is presented for illustration in fig. 1.

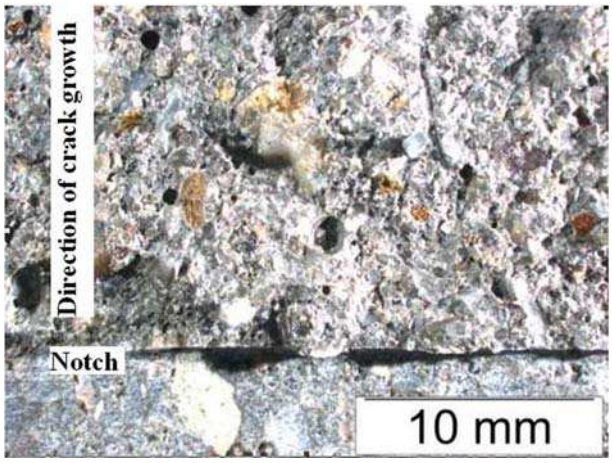

Fig. 1. The feature of the fracture surface of investigated material concrete BS 080405

2.2. Testing Procedures

The experimental data are carried out from the three-point bending (3PB) tests. Fig. 2. shows the geometry of the 3PB specimens. The 3PB specimen dimensions (in mm) were $L = 160$, $S = 120$, $W = 40$ and $t = 40$ for the first variant and $L = 400$, $S = 300$, $W = 100$ and $t = 100$ for the second one. The initial notch was made by a diamond saw that fabricated the 2–2.5 mm wide notches with controlled notch profiles and orientation. In this way 3PB, specimens with notch to width a_n/W ratios of about i) 0.33 were produced for subsequent static tests and ii) 0.10 were produced for subsequent fatigue crack growth testing.

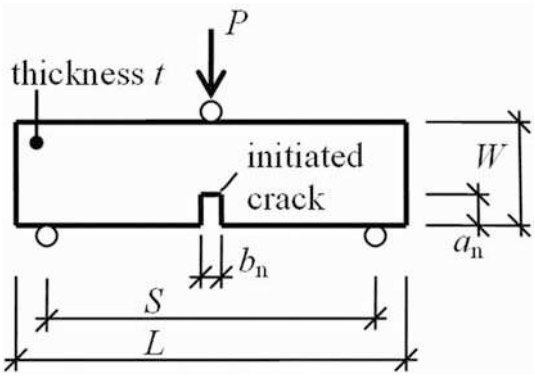

Fig. 2. The scheme of three-point bend (3PB) specimen geometry

The temperature and relative humidity were not controlled precisely. Nevertheless, both static and fatigue tests were carried out in laboratories where temperature and relative humidity values did not undergo significant fluctuations. The controlled values for temperature and relative humidity were 22 ± 2°C and 50 %, respectively.

2.3. Numerical modelling

For the correct evaluation of parameters obtained from experimental data a numerical study of the crack initiation and propagation in used 3PB specimens was carried out.

The influence of the initiation notch was investigated in Seitl et al. [15], Vesely et al. [22] and Seitl et al. [17] by means of a comparison of numerically simulated fracture process in the

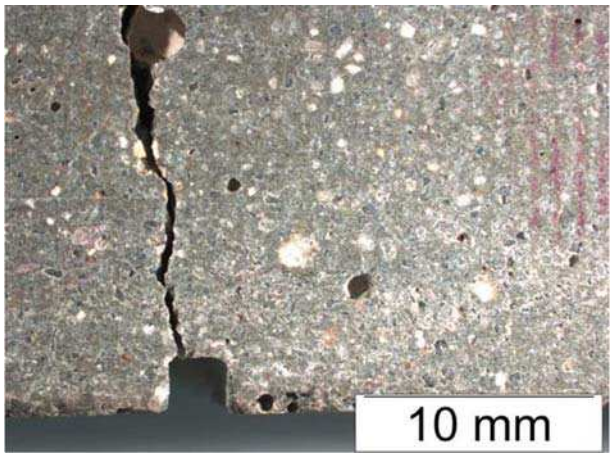

Fig. 3. Magnified view of the double V-notch created using a diamond disc saw. The crack is initiated at one corner of the starting notch and propagates throughout the specimen

cracked specimen and the specimens with the double V-notch of several widths. Typically, the crack initiated from the one of the rectangular notches, see fig. 3.

The numerical simulations of the fracture according to standard linear elastic fracture mechanics (LEFM) for cracks and generalized LEFM of general singular stress concentrators for notches were performed by finite element method (FEM) programs using ANSYS [1] and FRANC2D [7]. The FEM simulations were performed under plane strain conditions. All stresses were assumed to remain in the elastic range and the assumptions of LEFM were taken into account. Details are mentioned in e.g. Seitl et al. [16].

The explanation of the reasons for the application of LEFM (LEFM of general singular stress concentrators) within these analyses consists in the fact that the techniques of determination of fracture-mechanical properties of quasi-brittle materials (based on classical non-linear fracture models mentioned above) employ the approach of equivalent elastic crack, which essentially is the concept of LEFM supplemented with additional assumptions. The computational framework of LEFM is used both within the determination of effective crack models parameters (effective crack length or its extension, effective fracture toughness or effective toughness, i.e. fracture energy) and cohesive crack models (specific fracture energy, current – local – specific fracture energy). As these techniques work with the presumption that a crack (equivalent elastic, i.e. effective, but definitely no notch) is propagating in the loaded body, it is important to know how much the conditions (stresses, displacements) in the body differ in the cases where the initial stress concentrator is a crack or a notch. Since the length of the imaginary effective crack (or the crack extension) propagating from the concentrator tip is then calculated without regard to its shape (possibly together with the other fracture parameters appropriate to the models used, for which the effective crack length serves as an input) the values of such parameters can be substantially affected by this simplification, see details in Seitl et al. [15] and Veselý et al. [22].

The stress intensity factor range of the 3PB specimen for the propagation cracks is calculated as follows e.g. (Murakami et al. [10]):

$$\Delta K = \frac{3S\Delta P}{2tW^2}\sqrt{\pi a} f\left(\frac{a}{W}\right), \tag{1}$$

where S, t and W are characteristic sizes of the specimens/testing geometry, see fig. 2, ΔP is

the amplitude of the cyclic load, a is crack length and f is a dimensionless function of a/W that depends on the finite size of the specimen.

In the literature, e.g. (Tada at al. [21]), it is possible to find functions $f(a/W)$ for 3PB configuration for ratio $S/W = 4$ or 8. For specimen used here the ratio $S/W = 3$ and the dimensionless function $f(a/W)$ has to be calculated. The calculation was performed by finite element software ANSYS using the standard procedure KCALC. For $0.1 \leq a/W \leq 0.8$ the results obtained were expressed in the following approximation:

$$f\left(\frac{a}{W}\right) = 51.738\left(\frac{a}{W}\right)^4 - 47.98\left(\frac{a}{W}\right)^3 + 19.446\left(\frac{a}{W}\right)^2 - 2.387\,3\left(\frac{a}{W}\right) + 1.041. \quad (2)$$

Consequently, the values of the stress intensity factor range for used 3PB specimen were calculated from equation (2) in the following.

2.4. Static Tests

The static tests were carried out in a testing machine made by the Zwick/Roell Company. The deflection control was used; the loading rate was 0.05 mm/min. During tests a load-deflection diagram was recorded, see fig. 5. Effective fracture toughness was measured using the Effective Crack Model (see, [8, 18]). This model combines linear elastic fracture mechanics and the crack length approach. A three-point bending test of a specimen with a central edge notch is used in this approach [13]. Two nominal sizes of the beams are used $40 \times 40 \times 160$ mm and $100 \times 100 \times 400$ mm, the depth of the central edge notch is about 1/3 of the depth of the specimen (40 mm, 100 mm) and the loaded span are equal to 120 mm and 300 mm, respectively, see fig. 2.

2.5. Fatigue Tests

The fatigue crack growth experiments were carried out in a computer-controlled servo hydraulic testing machine (INOVA-U2). Fatigue testing was conducted under load control. Stress ratio $\sigma_{\min}/\sigma_{\max} = 0.1$ and 10 Hz frequency rate were adjusted in all monitored cases. Crack length was monitored on both sides using an optical microscope with resolution of 0.01 mm. Because the maximum size of aggregates was 4 mm, see subsection 2.1, the crack increment $\mathrm{d}a$ was larger than 4 mm. The 3PB fatigue test configuration is shown in the fig. 4, see ASTM [2] for details about measurement of fatigue crack growth rates.

As an important parameter to describe the fatigue rupture resisting ability of structures, fatigue crack propagation (FCP) rate $\mathrm{d}a/\mathrm{d}N$ is used to estimate the residual fatigue life. It can be seen that the FCP rate $\mathrm{d}a/\mathrm{d}N$ and the stress intensity range ΔK are related to each other. Many experimental results have shown that $(\mathrm{d}a/\mathrm{d}N)$–$\Delta K$ log-log curve can be for stable crack propagation (stage II) expressed in simple form [20]. Paris and Erdogan [11] first described the crack propagation phase. They found, by analyzing experimental data using regression analysis, for repetitive loading conditions that the crack propagation rate $\mathrm{d}a/\mathrm{d}N$ is:

$$\frac{\mathrm{d}a}{\mathrm{d}N} = C\Delta K^m \quad (3)$$

where C and m are experimentally determined parameters, $\Delta K = (K_{\max} - K_{\min})$ is the range of the stress intensity factor, a is the crack length, and N is a load excursion cycle. The law is mostly valid at stage II (stable crack propagation) and makes it possible to estimate the number of loading cycles to final fracture.

Another widely accepted approach for engineering practice is based on empirically derived S–N diagrams, also known as Wöhler curves. The S–N approach is still a useful tool to assess

Fig. 4. The three-point bending fatigue test configuration

fatigue failure of many modern structures that are subjected to repeated loading, where the applied stress is under the elastic limit of the material and the number of cycles to failure is large, see e.g. Farahmand et al in [6]. Fatigue test data can be provided to the analyst in tabular form or in the form of an S–N diagram. Along with data points, the two typical analytical expressions for the curves in the following form were obtained through linear regression:

$$\sigma_f = cN^d \tag{4}$$

or in the form

$$S_n = a \log N + b, \tag{5}$$

where σ_f / S_n is stress amplitude expression, N is cycle and c, d or a, b are the material parameters.

3. Results and Discussion

3.1. Results from Static Tests

Experimental static load-deflection curves (l–d diagrams) were used and for specimen size $100 \times 100 \times 400$ mm are displayed in fig. 5. Every curve was assessed separately, and the variability of the effective fracture toughness is described by the estimation of the first two statistical moments (mean value and standard deviation) – see table 2.

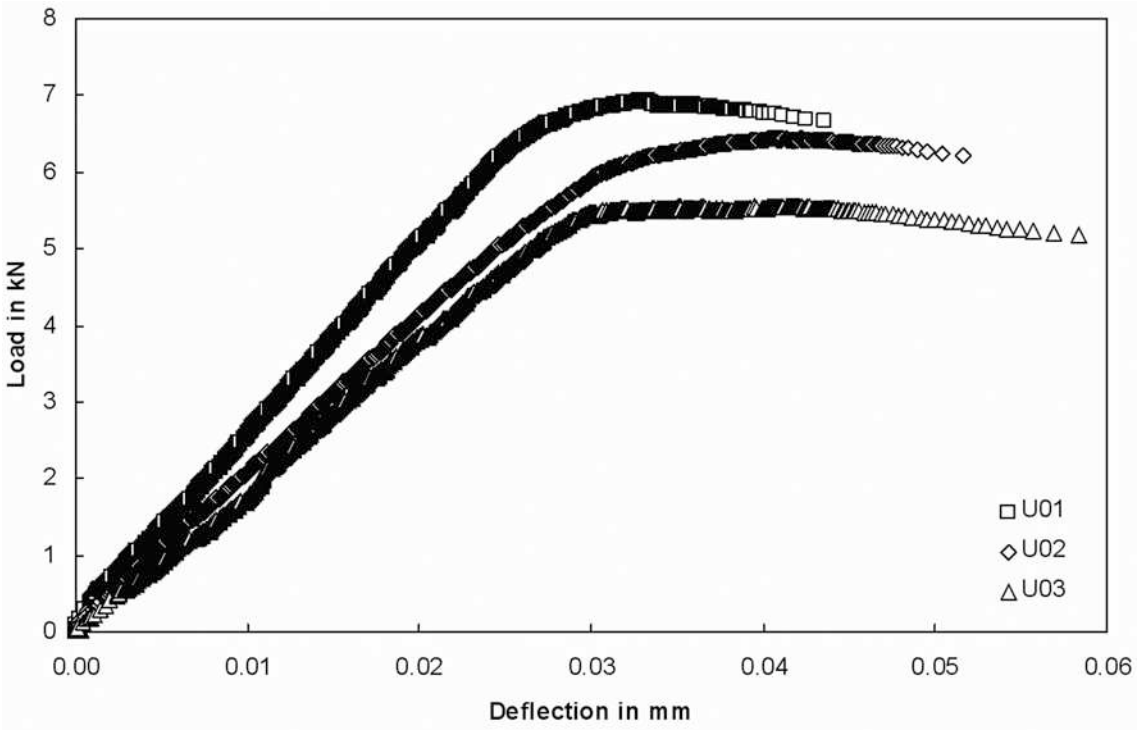

Fig. 5. Load-deflection diagram of BS 080405 under three-point-bending static test

Table 2. Results of static tests: parameter value, mean value, standard deviation and coefficient of variation

Specimen	Value $[\mathrm{MPa}\cdot\mathrm{m}^{1/2}]$	Mean Value $[\mathrm{MPa}\cdot\mathrm{m}^{1/2}]$	Standard Deviation $[\mathrm{MPa}\cdot\mathrm{m}^{1/2}]$ (COV [%])
BS080405_U01	1.190	1.161	0.086 (7.4)
BS080405_U02	1.229		
BS080405_U03	1.064		

3.2. Results from Fatigue Tests

The result of the fatigue crack growth tests performed at stress ratio $\sigma_{\min}/\sigma_{\max} = 0.1$ using the 3PB specimen geometries for material BS 080405 are presented in figs. 6–8 and in table 3. Note that the fatigue test data of material BS 080405 show considerable scatter because of the random orientation of fibres.

3.2.1. Fatigue Crack Growth Rate – $\mathrm{d}a/\mathrm{d}N$–ΔK

The fig. 6 shows the dependence of the fatigue crack propagation rate $\mathrm{d}a/\mathrm{d}N$ on the stress intensity factor range ΔK in the region of the Paris law (equation (3)) validity. From the Paris equation, the relationship of $\log(\mathrm{d}a/\mathrm{d}N)$ and $\log \Delta K$ can be obtained,

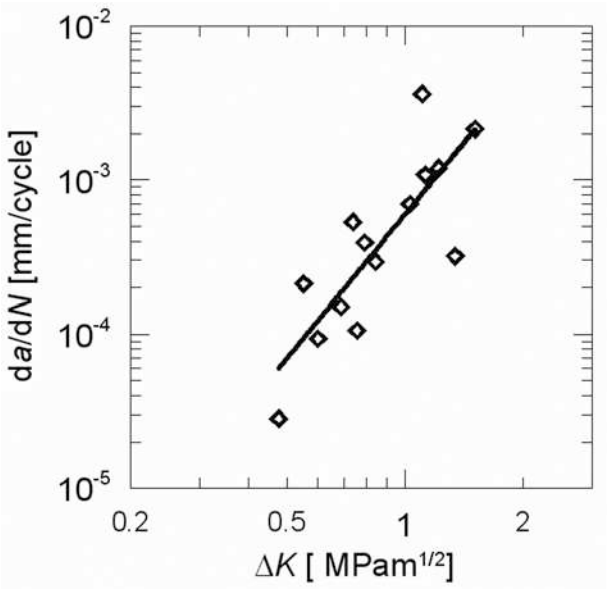

Fig. 6. Fatigue crack growth rate data obtained for concrete BS 080405

$$\log\left(\frac{\mathrm{d}a}{\mathrm{d}N}\right) = \log C + m \log \Delta K \tag{6}$$

In log-log grid, it is expressed as a straight line with the intercept $\log C$ and slope m. At stage II (stable crack propagation), a line segment was used for linear fitting. Linear fit parameters of experimental data at crack steady growth stage gives values $C = 6 \cdot 10^{-4}$ and $m = 3.100\,6$, respectively index of dispersion is $R^2 = 0.66$.

3.2.2. Wöhler Curve

The results of the fatigue tests under varying maximum bending stress level are summarized in fig. 7. where maximum bending stress in the fatigue experiment is plotted against the logarithm of number of cycles to failure. Along with data points, the analytical expressions for the curves (in the form $\sigma_f = cN^d$) were obtained through linear regression. The regression equation and the regression coefficient for the present tested material are $\sigma_f = 5.84N^{-0.033\,3}$ and $R^2 = 0.74$ (index of dispersion).

As it was mentioned in table 1, the tested material is considered in the range of high cycle fatigue, therefore an upper limit on the number of cycles to be applied was selected as 2 million cycles. The test was terminated when the failure of the specimen occurred or the upper limit of loading cycles was reached, whichever occurred first.

Finally, let's compare the linear regression lines for the present and the literature found results for 3PB tests. The literature results were taken from [9], where authors (Lee and Barr) provide an overview of recent developments in study of the fatigue behaviour of plain and fibre reinforced concrete. They consider three kinds of concrete plain and reinforced by steel fibre with 0.5 % and 1 % fibre content.

The results of these tests are recorded in a Wöhler diagram, see fig. 7. where on one axis the normalized stresses ($S_n = \sigma_f/\sigma_s$; σ_f – the values of fatigue loading stress and σ_s – values of static maximal stress) is given and on the other axis the numbers of cycles until failure on log scale are presented. The Wöhler curves coefficients for analytical expression in the form

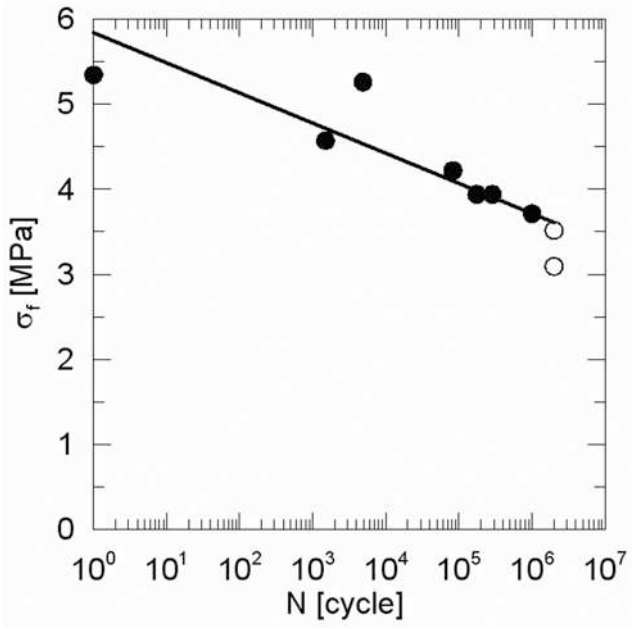

Fig. 7. Wöhler diagram (σ_f–N curve) obtained from measurement of concrete BS 080405

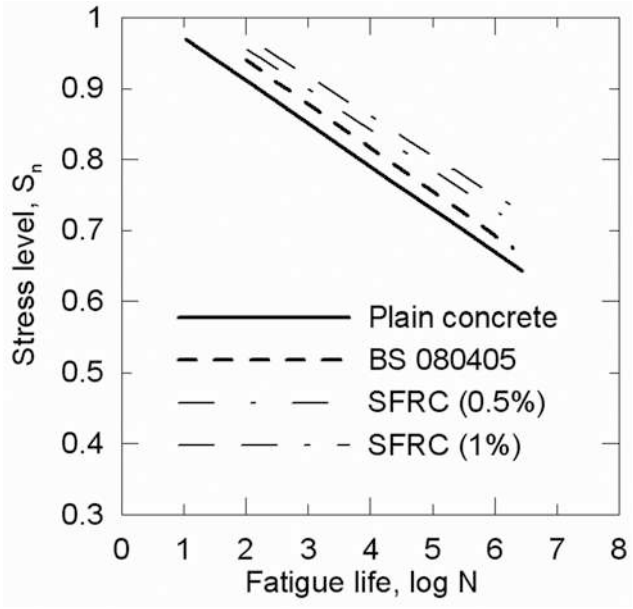

Fig. 8. Comparison between S_n–N curves for plain concrete, SFRC (0.5 % and 1.0 % fibre content) from [9] and presented results for BS 080405

$S_n = a \log N + b$ equation (5) are presented in table 3. The indexes of dispersion R^2 are in the last column.

The fatigue life increases with a decrease in the amplitude of the loading cycle. Moreover, it can be seen that for small values of N, the S_n–N curves tend to converge to σ_f values that are greater than the static value $N = 1$. This is mainly because the compressive strength used as a reference was obtained from static tests in which the loading rate is much lower than that of the fatigue tests.

Table 3. Coefficients of S_n–N curves and indexes of dispersion

Material	a and b in the fatigue equation		R^2
	a	b	
Plain concrete	$-0.060\,6$	$1.032\,7$	$0.724\,3$
BS 080405	$-0.061\,7$	$1.063\,2$	$0.744\,4$
SFRC (0.5 %)	$-0.057\,5$	$1.072\,7$	$0.606\,2$
SFRC (1 %)	$-0.055\,9$	$1.085\,4$	$0.730\,9$

There appears to be significant benefit derived from the addition of fibres. It can be seen the improvement of fatigue life due to fibre content increase from 0 % to 0.2 % and is comparable with improvement due to increase of fibre content from 0.5 % to 1 %.

4. Conclusions

The basic fracture mechanics parameters of advanced building material BS 080405 – glass fibres reinforced cement based composite – were measured. To this aim three-point bend specimens with starting double V-notch were prepared and tested under static and cyclic loading. To evaluate the results the finite element method was used for the estimation of the corresponding values of stress intensity factor for the 3PB specimen used.

From experimental tests on 3PB specimens made from concrete BS 080405, the following conclusions can be drawn:

1. Effective fracture toughness values about $1.2\ \mathrm{MPa}\cdot\mathrm{m}^{1/2}$ from static fracture tests are slightly higher compared with typical values of this type of composite without fibres (0.8–1.0 $\mathrm{MPa}\cdot\mathrm{m}^{1/2}$).

2. The fatigue behaviour characterized by $\mathrm{d}a/\mathrm{d}N$ versus ΔK values was obtained in the region of fatigue stable crack propagation and represented by Paris equation (3) with parameters ($C = 6\cdot 10^{-4}$, $m = 3.100\,6$).

3. The S–N curve for the material studied has been presented in terms of linear relations between the maximum stress level σ_f and N in the form $\sigma_f = 5.84N^{-0.033\,3}$, where N is the fatigue life in cycles.

4. The results obtained should contribute to a more reliable estimation of service life of structures/elements.

5. Authors suppose further directions of the research: i) Finding of correlation fatigue and fracture characteristics with the technological influences; ii) Numerical simulation/prediction of the cracking of material due to variable–amplitude loading.

Acknowledgements

The work has been supported by the grant project GA CR 103/08/0963 from the Czech Science Foundation and research project AV OZ 20410507.

References

[1] ANSYS, Users Manual Version 10.0, Swanson Analysis System, Inc., Houston, Pennsylvania (2005).

[2] ASTM, Standard E 647–99: Standard Test Method for Measurement of Fatigue Crack Growth Rates, 2000 Annual Book of ASTM Standards, Vol. 03.01, (2000) 591–630.

[3] Baluch, M. H, Qureshy, A. B., Azad, A. K., Fatigue crack propagation in plain concrete, SEM/RILEM International Conference on Fracture of Concrete and Rock, Houston, 1987.

[4] Bazant, Z. P., Shell, W. F., Fatigue fracture of high-strength concrete and size effect, ACI Materials Journal, 90 (5), (1993) 472–478.

[5] Bazant, Z. P., Xu, K., Size effect in fatigue fracture of concrete, ACI Materials Journal, 88 (4), (1991) 390–399.

[6] Farahmand, B., Bockrath, G., Glassco, J., Fatigue and fracture mechanics of high risk parts, Chapman & Hall, 1997.

[7] FRANC2D A Crack Propagation Simulator for Plane Layered Structures, http://www.cfg.cornell.edu.

[8] Karihaloo, B. L., Fracture mechanics of concrete, New York: Longman Scientific & Technical 1995.

[9] Lee, M. K., Barr, B. I. G., An overview of the fatigue behaviour of plain and fibre reinforced concrete, Cement & Concrete Composites, 26, (2004) 299–305.

[10] Murakami, Y., et al., Stress Intensity Factor Handbook I, II, III, Pergamon Press, Oxford, 1987.

[11] Paris, P., Erdogan, F., A critical analysis of crack propagation laws, Journal of Basic Engineering, Transactions of the American Society of Mechanical Engineers, 85, (1963) 528–534.

[12] Perdikaris, P. C., Calomino, A. M., Kinetics of crack growth in plain concrete, SEM/RILEM International Conference on Fracture of Concrete and Rock, Houston, 1987.

[13] RILEM, Committee FMC 50 (Recommendation), Determination of the fracture energy of mortar and concrete by means of three-point bend test on notched beams, Materials and Structures, 18, (1985) 285–290.

[14] Seitl, S., Kersner, Z., Routil, L., Knesl, Z., Selected Fatigue and Fracture parameters of glass fiber cement based composite, 8th International Symposium on Utilization of High-Strength and High-Performance Concrete, 27–29 October 2008 Tokyo Japan, (2008a) (On CD).

[15] Seitl, S. Klusák, J., Keršner, Z., "Influence of notch width and length on crack initiation in 3PB specimens", Engineering mechanics 2008, (2008b) 807–811.

[16] Seitl, S., Klusák, J., Keršner, Z., The influence of a notch width on a crack growth for various configurations of three-point bending specimens, Materials Engineering, 14 (3), (2007) 213–219 (in Czech).

[17] Seitl, S., Řoutil, L., Klusák, J., Veselý, V., The influence of the shape of a saw-cut notch in quasi-brittle 3PB specimens on the critical applied force, Applied and Computational Mechanics, 2 (1), 2008 123–132.

[18] Shah, S. P., High Performance Concrete: Strength vs. Ductility and Durability, In: Proceedings of the Symposium on Non-Traditional Cement and Concrete, Bílek, V. and Keršner, Z. (eds.), Brno, (2002) 347–358.

[19] Slowik, V., Plizzari, G., Saouma, V., Fracture of concrete under variable amplitude loading, ACI Materials Journal, 93 (3), (1996) 272–283.

[20] Suresh, S., Fatigue of Materials, Cambridge University Press, Cambridge, 1998.

[21] Tada, H., Paris, P. C., Irwin, R. G., The Stress Analysis of Cracks Handbook (Hardcover), ASM International; 3rd edition, 2000.

[22] Veselý, V., Keršner, Z., Seitl, S. Klusák, J., Influence of notch width on fracture response of bended concrete specimens, Engineering mechanics 2008, (2008) 1 113–1 120.